NORSAR

NORSAR Scientific Report No. 1-2001

Technical Summary

1 October 2000 - 30 June 2001

Frode Ringdal (ed.)

Kjeller, July 2001

6.4 Automatic reprocessing of events from the Khibiny Massif

6.4.1 Introduction

In the early 1990's NORSAR scientists developed and tested a procedure for two-step location of seismic events recorded by a regional network (see e.g. Kværna and Ringdal, 1994). At the time, this processing was applied experimentally to seismic events in the Khibiny Massif, Kola Peninsula. However, no attempt was made to use this method in a practical day-to-day monitoring situation, and also, it was not applied to any other regions.

We have recently made an effort to return to this location procedure, with the aim to apply it in a more general context and also to investigate options for practical routine implementation of the method. This paper gives a summary of the method as originally developed, and attempts to set up a possible system for automatic, routine processing that could be expandable to a more general case.

We first note that in order to obtain an accurate location of a seismic event by using a regional network, we need as precise as possible estimates of onset times, azimuths and slownesses, of the different seismic phases at each station or array.

In this study we first investigate the use of an onset-picker to be used for different seismic phases. The onset-picker is based on an autoregressive (AR) model to express the seismic signals, and Akaike's information criterion (AIC) for identifying arrival times for seismic waves, see GSE/JAPAN/40 (1992) for details. Further we will apply FK-analysis to derive more consistent azimuth and slowness values for the new onset time (see Kværna and Doornbos, 1986), and then we will do a relocalization of the event (see Schweitzer, 2001).

At NORSAR, a two-step procedure has been in use since 1985, to determine onset times for different seismic phases, see Mykkeltveit and Ringdal (1981) and Mykkeltveit and Bungum (1984) for details. A fully automated processing, from onset picking to localization, has since then been developed by Ringdal and Kværna (1989) and is now routinely applied to the seismic signals available at NORSAR. This Generalized Beamforming (GBF) system for processing of seismic events gives a daily bulletin with origin times, onset times, location and so on. We will refer to this daily bulletin as the GBF-list, see Kværna (1990, 1994) for details about the GBF system.

The GBF system provides us with initial signal processing information of the stations available at NORSAR, with phase association and localization of seismic events. To obtain more accurate locations, we have to improve the accuracy of the onset times, slowness and azimuth estimates. We also need to have a more correct phase identification, and a more accurate local velocity model for the different seismic phases. In addition, systematic biases in azimuth, slowness and traveltimes of the different seismic phases will be removed by introducing corrections for events in the actual region. For events in the Khibiny Massif, we would also like to include data from the Apatity three-component station (APZ9), which is currently not being used by the GBF system.

Region-specific application

We want to apply the approaches described in the previous paragraph to a specific area with recurring seismicity. From this area we will select a dataset with typical features for the seismicity, analyze it with respect to the methods, and then find characteristics which can be used later to monitor this specific area. In the monitoring, the region-specific methods will be activated when an event in the GBF-list is located close to this area. Then the special characteristics will be used to improve the onset times and the FK-analysis, and thus hopefully improve the relocalization.

The Khibiny Massif events

We will consider seismic events from the mining region in the Khibiny Massif in the Kola peninsula of northwestern Russia (See Kremenetskaya, 1992, Kremenetskaya and Trjapitsin, 1995). This is an alkaline intrusion occupying about 1300 square kilometers (36 by 45 km) and rising about 1000 meters higher than the surrounding plain of the Kola peninsula. Six large mines are operated by the Apatit Joint Stock Company in the Khibiny Massif to supply products to the superphosphate and aluminum industries. Through our contact with the Kola Regional Seismological Centre, we have been provided with the exact locations of 36 seismic events in this region. The 36 mining events are described in more detail in Kværna (1993), otherwise we refer to Mykkeltveit (1992) and Kværna and Ringdal (1994) for more background information.

From the GBF-list we have derived initial locations, onset times, phase associations, azimuth and slownesses for all the 36 events. In a time window around the initial onset time, we will use the onset-picker to find a new onset time. The time window is based upon the initial onset time from the GBF-list, and/or predicted travel times for seismic phases from the mining region. Thus we search for a new onset time in a small time window where we assume the different seismic phases will arrive. We can then avoid erroneous phase associations. Around this new onset time, we will make a new FK-analysis to derive better azimuth and slowness values.

From this processing of our 36 events, the "ground truth" data, we establish local corrections for the travel times of the different phases, and also for the slowness and the azimuth. Then we do a relocalization of the seismic events, and compare them to the known locations.

6.4.2 Processing flow

The processing steps involved in picking new onset times are given in Fig. 6.4.1.

For each day we will search through the GBF-list to find the events initially located in the relevant region (the mining area of the Khibiny Massif). From the GBF-list we derive initial onset times for the different phases, azimuth and slowness/velocity. The data processing is done with the EP program, see Fyen (1989), and the relocalization is made by Hyposat, see Schweitzer (2001). For each phase the general processing is:

For the Apatity and the ARCES arrays, the first step is to form a beam in accordance with the initial parameters from the GBF-list. For signals from the Apatity three-component station, we will rotate the seismic traces in accordance with the parameters from the GBF-list if we are searching for a S-phase, else we will only use the z-component trace.

In a next step we will define a bandpass filter for the processing. This filter is phase dependent, and is found from initial testing of different signals from the Khibiny Massif. Further we will define a SNR computational interval, and the search interval for the AR-AIC method. All these intervals are based on initial testing and viewing of the data.

The data are filtered in the bandpass filter band, and the SNR is calculated. If the SNR is lower than 30, we will decimate the sampling rate of the signal to obtain better performance of the AR-AIC method.

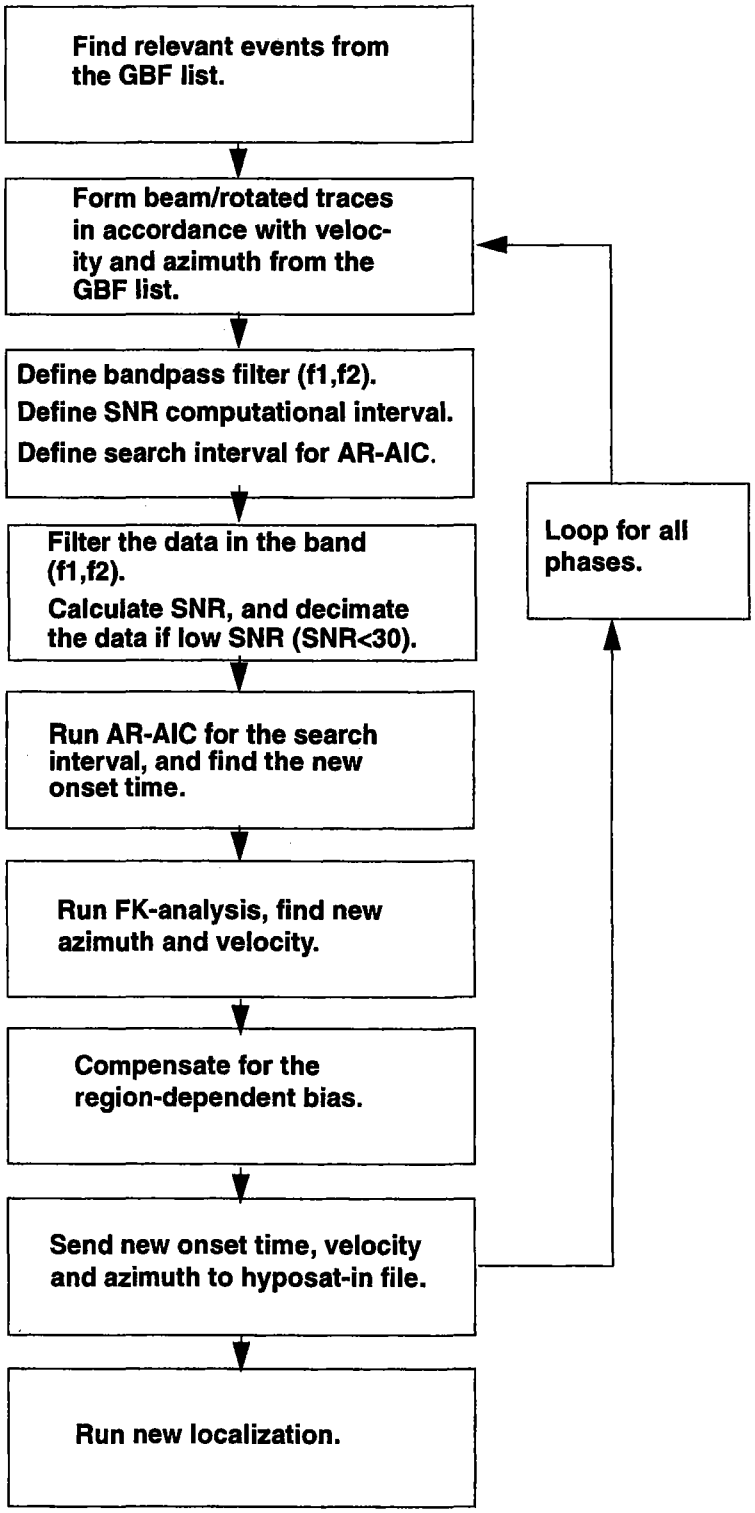

Fig. 6.4.1. Flowchart of steps involved in the automatic time picking algorithm.

The AR-AIC method is run in the search interval, with the onset from the GBF-list as an initial value. The new onset is picked.

Around the new onset, we run an FK-analysis, and new slowness/velocity and azimuth are derived.

A local model for corrections of traveltime, slowness and azimuth are introduced.

The new onset time, slowness and azimuth are sent to a Hyposat input file. When we have processed all phases for the three stations, the relocalization is made using Hyposat (Schweitzer, 2001), and the Hyposat output file gives the new localization, with an error ellipse.

6.4.3 Autoregressive model for determining onset times for seismic phases

In the processing we have used an autoregressive (AR) model for determining the different onset times of the different seismic phases. The method is described in GSE/JAPAN/40 (1992) and Yokota et al (1981), and thus we will not go into details about it in this text.

The seismic waves are described by an autoregressive (AR) model. Then Akaike's information criterion (AIC) is used to find the order and criterion for identifying onset times. The Akaike's information criterion is given by the equation:

AIC = - 2 (logarithmic likelihood) + 2 (number of parameters)

From the GBF-list we find an initial onset time for the different phases. Then the AR coefficients for both the noise and the seismic signal are derived from data in two different windows. The noise window is located in front of the initial onset, and the seismic signal window is located within the signal. We filter the data with two prediction error filters, and then the AIC criterion is derived from the filtered signal. The minimum of the AIC curve is taken to be the optimal division point between the noise and the seismic signal, and will thus be the new onset time for the seismic phase.

In the processing we have to decide the order of the autoregressive model (usually set to 8), the initial starting time (from the GBF-list), the length of looking back from the starting time (to find the AR-noise model), the length of window for deriving the AR-coefficients, and the total length of the AR-AIC window.

6.4.4 Derivation of processing recipes from the "ground truth" data

The "ground truth" data

The "ground truth" data come from underground explosions in six mines in the Khibiny Massif (the Apatity area on the Kola Peninsula of Russia). See Mykkeltveit (1992) for a detailed description of the mines and the mining activity. The center location of the mines are given in Table 6.4.1, and the locations can also be seen in Fig. 6.4.5 (the map). Mine no. I consists of both an underground part and an open-pit part.

Table 6.4.1. Center location of Khibiny mines

Mine	Latitude	Longitude
I, under-ground	67.670	33.728
I, open-pit	67.665	33.744
II	67.647	33.761
III	67.631	33.835
IV	67.624	33.896
V	67.632	34.011
VI	67.665	34.146

The exact sizes of these mines are not exactly known, but are assumed to be about 1 km^2. From a list of mining explosions, we have chosen 36 events with locations in the six mines, but where we do not know the exact origin time. The distance range from the mining region to the Apatity array (APA0), and the Apatity three-component station (APZ9), is from 18 to 49 km. The distance range to the ARCES array is about 400 km for all mines.

For each of the events we see clear Pg, Lg and Rg arrivals in the seismograms from both the Apatity array (APA0) and the Apatity three-component station (APZ9). For the ARCES array, we see clear Pn, Sn and Lg phases in the seismograms for all the mining events. Typical seismic signals from the Khibiny Massif at the different stations are given in Figs. 6.4.2 to 6.4.4.

The Khibiny Massif events

We have selected 36 events from the mining region in the Khibiny Massif. The initial locations of the events are found from the GBF-list, and are shown in Table 6.4.2, and seen in Fig. 6.4.5.

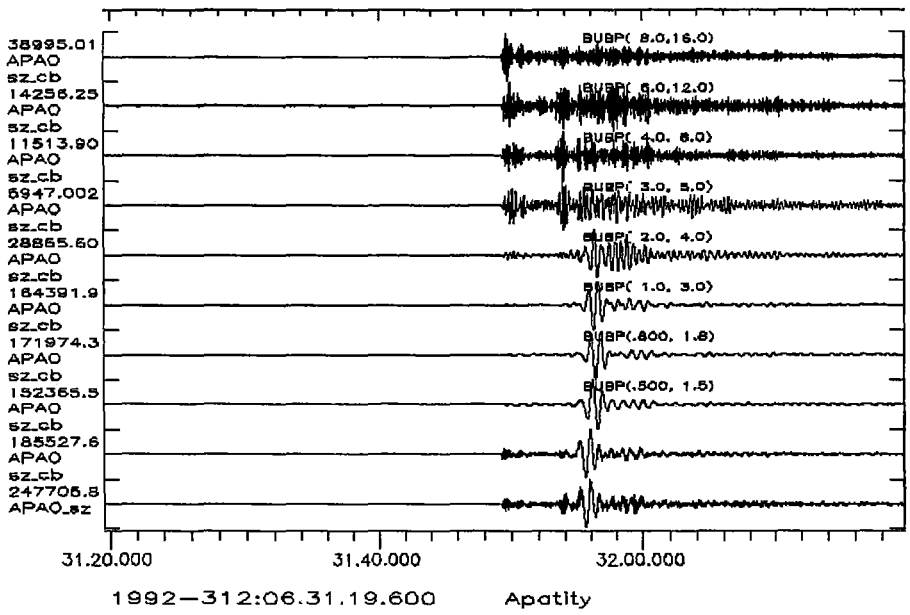

Fig. 6.4.2: The figure shows signals from the Apatity array. We have formed a P-beam in accordance with the parameters from the GBF-list for this event. The trace at the bottom is the unfiltered APA0_sz seismogram, and the one above is the unfiltered beam from all the z-component traces in the array. We have filtered the beam in different bandpass frequencies; 0.5-1.5, 0.8-1.8, 1.0-3.0, 2.0-4.0, 3.0-5.0, 4.0-8.0, 6.0-12.0, 8.0-16.0 Hz.

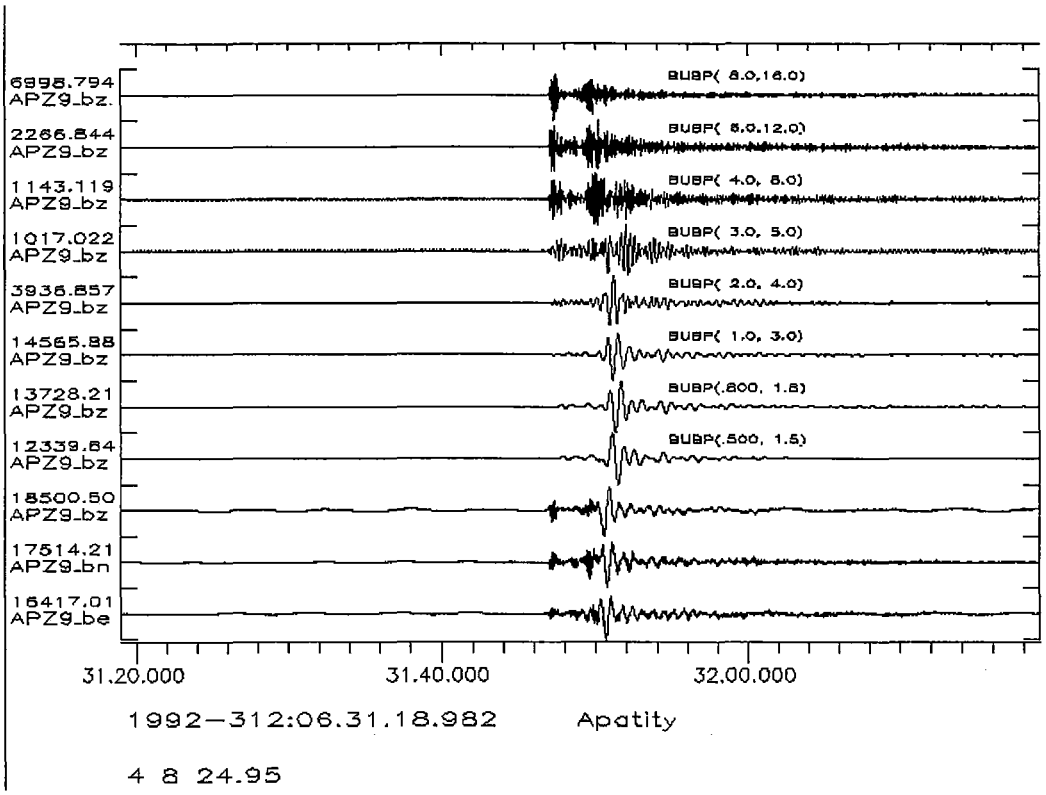

Fig. 6.4.3: The figure shows seimograms from the Apatity three-component station, APZ9. The three bottom traces show the unfiltered signal from the APZ9_bz, APZ9_be and APZ9_bn components. The remaining traces show the APZ9_bz seismogram filtered in the same set of frequency bands as in the previous figure (6.4.2).

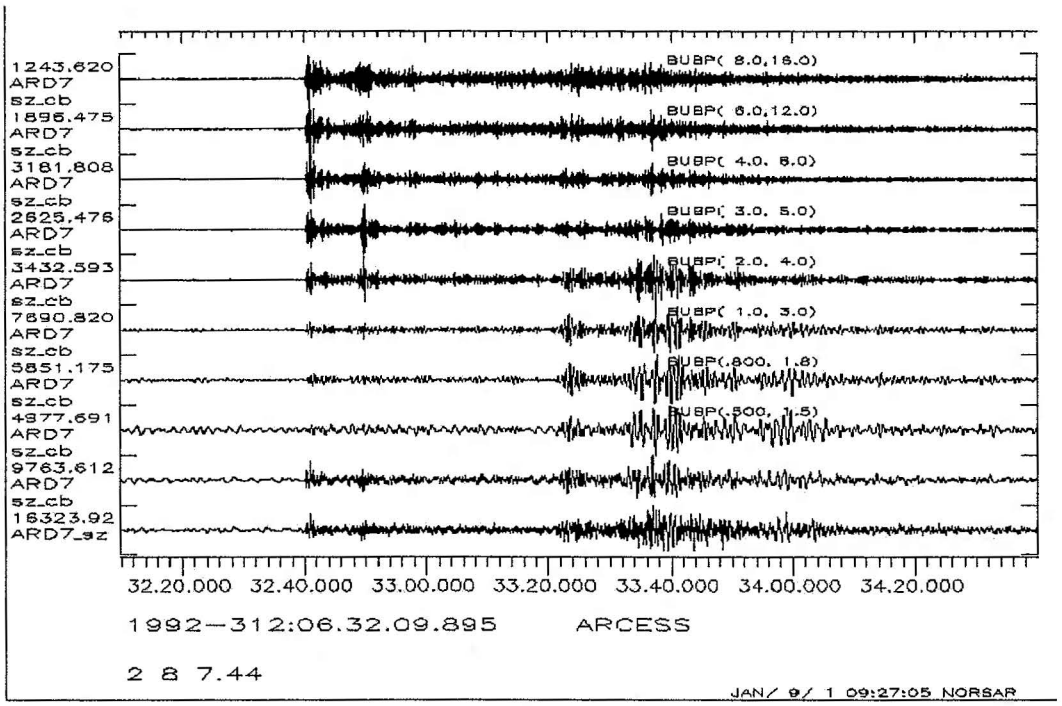

Fig. 6.4.4: The figure shows recordings at the ARCES array. The bottom trace is the unfiltered seismogram for the site ARD7_sz; the one above is the unfiltered P-beam from all the z-components in the array, and the remaining traces show the beam filtered with the same frequency bandpass filters as in the two preceding figures.

Table 6.4.2. GBF locations of the 36 mining events from the Khibiny Massif, with location errors (red) in kilometers.

Mine 1	Mine 2	Mine 3	Mine 4	Mine 5	Mine 6
Lat Lon Err (km)	Lat Lon Err (km)	Lat Lon Err (km)	Lat Lon Err (km)	Lat Lon Err (km)	Lat Lon Err (km)
67.75,34.44,31.4	67.60,34.26,21.8	67.35,34.67,47.5	67.45,34.70,39.4	67.45,34.70,35.7	67.75,33.91,13.8
67.75,34.70,42.1	67.75,34.70,41.4	67.60,34.26,18.4	67.45,33.92,19.4	67.75,34.44,22.4	67.45,34.97,42.5
67.75,34.44,31.4	67.75,34.70,41.4	67.45,34.70,42.0	67.45,34.70,39.4	67.45,34.70,35.7	67.75,34.70,25.3
67.45,34.70,39.0	67.45,34.70,45.6	67.45,35.75,84.1	67.75,34.70,36.9	67.60,34.26,11.2	67.75,34.70,25.3
67.60,33.47,13.7		67.75,34.70,39.0	67.45,34.44,30.2		67.45,34.70,33.7
67.75,33.91,11.8			67.45,33.92,19,4		67.75,34.44,15.6
67.75,34.70,41.6			67.55,35.52,69.6		
67.75,34.16,20.0			67.45,34.70,39.4		
67.75,34.70,41.6					

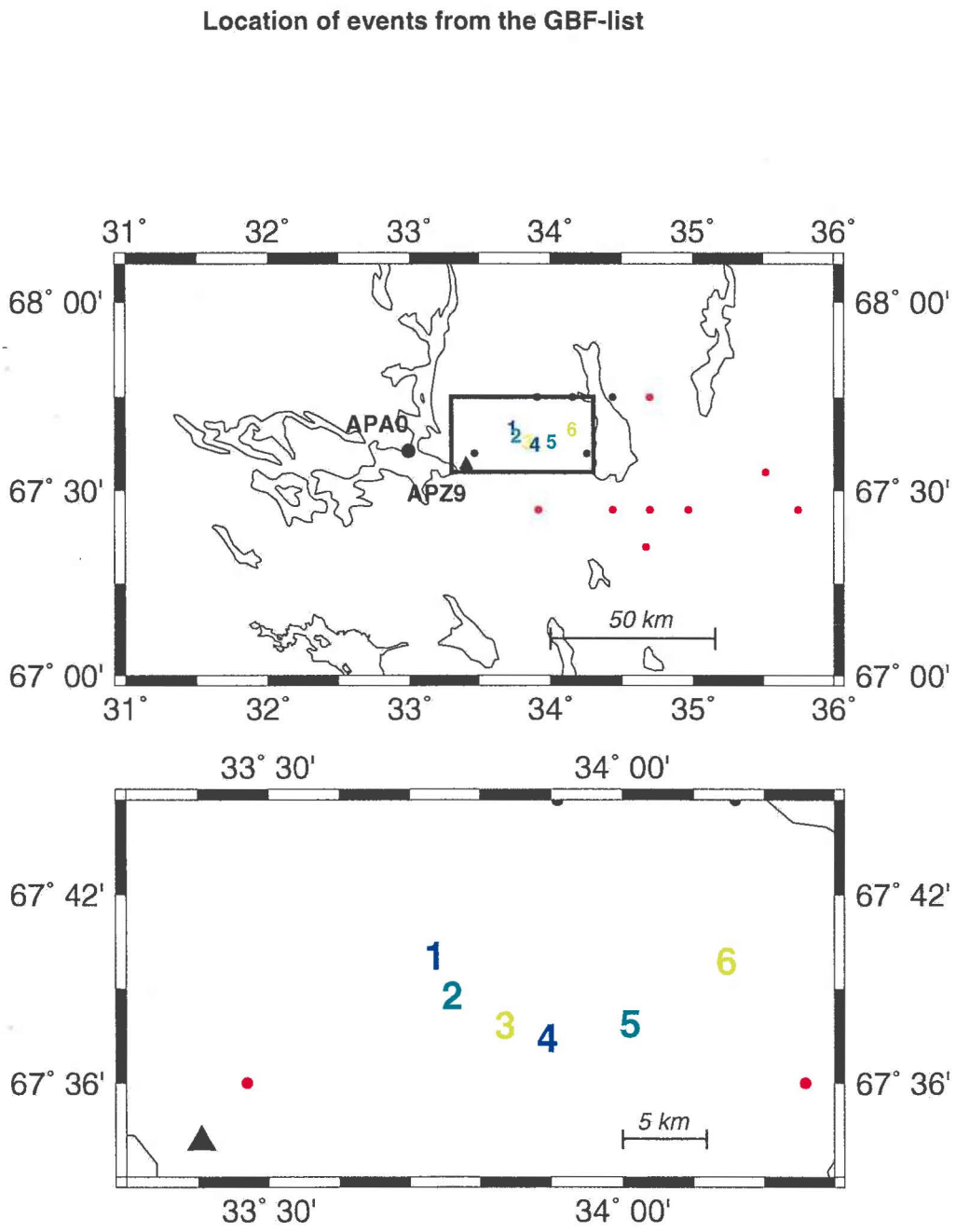

Fig. 6.4.5. Map showing the locations of the 36 events as given in the GBF list. The bottom part is an expanded view showing the locations closest to the 6 mines (numbered 1 to 6).

Determination of the onset time when GBF data are missing

As mentioned earlier in this contribution, the GBF system does not use data from the Apatity three-component station (APZ9) in the processing. Thus we have no initial onset, azimuth and slowness for the Pg and Lg phase from this station.

Since we need the initial data for the Apatity three-component station (APZ9) in the processing, we will have to establish a model for finding estimates for the data. First we have calculated the azimuth from the center point of the mining area to the three-component station. Then we have subtracted this azimuth from the backazimuth for the Apatity array (APA0) found earlier in the processing. This difference is called "azimuth_difference" in the following equations. The distance between the Apatity three-component station and the Apatity array was calculated, and the velocity for Pg and Lg phases in the Apatity area was derived from a local traveltime model. Thus we could find the approximate time difference for signals reaching the three-component station and the array, both for Pg and Lg phases. The time difference for a Pg phase is thus given by:

time_difference_Pg = distance_between_stations*cos(azimuth_difference)/velocity_Pg

and the time difference for a Lg phase is given by:

time_difference_Lg = distance_between_stations*sin(azimuth_difference)/velocity_Lg

To find the initial Pg onset time, we now subtracted time_difference_Pg from the new Pg onset time found from the Apatity array (APA0) processing. The initial Lg onset time was found in the same way. In this way we had established initial onset times to be used later in the processing, for the relevant phases at the Apatity three-component station (APZ9).

Determination of origin time for the reference events

Since we did not know the origin times of the reference events, we had to establish a model to find them. For each of the 36 events, we used the new Pg onset time for the Apatity three-component station, APZ9. This is the station closest to the mining area, thus the seismic waves will have the shortest path to travel. We assume that the influence of an erroneous traveltime model is less for this station and this phase than for other phases and stations. From this onset time and the distance from the station to each mine, the origin time for each event could be found using a local traveltime model. This origin time was later used to find local corrections for traveltimes, azimuth and velocity.

6.4.5 Processing details for the different stations

We have derived a set of parameters for each station we use in our processing (the Apatity array (APA0), the Apatity three-component station (APZ9), and the ARCES array). As outlined earlier in this text, these parameters are derived from initial testing and viewing of the data.

In the next (sub)paragraphs we will outline the parameters for each station and phase. The following descriptions is a general outline of the use of each parameter:

- The trace(s) used in the processing: For the Apatity array and the ARCES array, the traces used are the P- or the S-beam of the z-component channels in the arrays. For the Apatity three-component station, when processing the P phase, we use the z-component, and when processing the S phase, we use the rotated, transverse component.
- The initial azimuth and slowness is read from the GBF-list, predicted from a local traveltime model, or is derived from a FK-analysis of other (earlier) phases.
- The initial onset time is read from the GBF list, or predicted from local traveltime models based on the GBF locations.
- The time window to search for the maximum SNR is defined around the initial onset from the GBF-list or derived from local traveltime models.
- A (Butterworth) bandpass filter is applied to filter the seismic traces prior to running the AR-AIC method. The bandpass filter is usually fixed for all events.
- The parameters for the AR-model are: time window for calculations of the AR-coefficients, the time length to look back from initial time point, and the total length of the AR-window.
- The parameters for the FK-analysis are: time window around the initial onset, maximum slowness, and the chosen frequency range.

Processing details for the Apatity array, Pg phase

- SNR time window: +/- 3.0 seconds around the initial onset.
- Bandpass filter: 4 - 8 Hz.
- AR-coefficients' time window: 4.0 seconds. The time length to look back: 7.0 seconds. Total length of the AR-window: 10.0 seconds.
- FK time window: 0.3 seconds before, and 2.0 seconds after the new Pg onset. Maximum slowness: 0.4.

Processing details for the Apatity array, Lg phase

- SNR time window: From + 2.0 seconds after the new Pg onset to + 5.0 seconds from the initial Lg onset time.
- Bandpass filter: 2 - 8 Hz.
- AR-coefficients' time window: 3.0 seconds. The time length to look back: the time difference between the initial Lg onset, and the new Pg onset, minus 0.5 seconds. Total length of the AR-window: the time difference between the initial Lg onset, and the new Pg onset, plus 3.0 seconds

- FK time window: 0.4 seconds before, and 3.0 seconds after the new Lg onset. Maximum slowness: 0.4.

Processing details for the Apatity array, Rg phase

- The peak of the Rg phase was identified from the STA envelope created from z-component data. Bandpass filter: 0.8 - 2.0 Hz.
- The start of the STA envelope was set 1.0 second after the new Pg onset time, and the length was set to 19.0 seconds.
- FK time window: 1.5 seconds before, and 1.5 seconds after the peak of the Rg phase. Maximum slowness: 0.6.

Processing details for the Apatity array 3-component reference site (APA0), Lg phase

- SNR time window: + 2.0 seconds after the new Pg onset, to + 5.0 seconds from the initial Lg onset time.
- Bandpass filter: 2 - 8 Hz.
- APA0_hn and APA0_he were rotated with the azimuth found from the FK-analysis of Pg from the Apatity array.
- AR-coefficients' time window: 3.0 seconds. The time length to look back: the time difference between the initial Lg onset, and the new Pg onset, minus 0.5 seconds. Total length of the AR-window: the time difference between the initial Lg onset, and the new Pg onset, plus 4.0 seconds
- FK time window: 0.5 seconds before, and 3.0 seconds after the new Lg onset. Maximum slowness: 0.2, and alpha was set to 6.0, beta was set to 3.46.

The Lg data from the processing of the Apatity array 3-component central station, APA0, were not used in the relocalization. It is included here because it might be interesting to see if onset, azimuth and slowness from this station are more consistent than the results from Lg-phase processing using the full Apatity array.

Processing details for the Apatity 3-component station APZ9, Pg phase

- SNR time window: +/- 3.0 seconds around the initial onset.
- Bandpass filter: 4 - 8 Hz.
- For the processing we used the APZ9_bz component, no rotation of the trace.
- AR-coefficients' time window: 1.5 seconds. The time length to look back: 7.0 seconds. Total length of the AR-window: 10.0 seconds.
- FK time window: 0.5 seconds before, and 2.0 seconds after the new Pg onset. Maximum slowness: 0.2, and alpha was set to 6.0, beta was set to 3.46.

Processing details for the Apatity 3-component station APZ9, Lg phase

- SNR time window: + 2.0 seconds after the new Pg onset, to + 5.0 seconds from the initial Lg onset time.

- Bandpass filter: 2 - 8 Hz.
- APZ9_bn and APZ9_be were rotated with the azimuth found from the FK-analysis of Pg from APZ9_bz.
- AR-coefficients' time window: 1.5 seconds. The time length to look back: the time difference between the initial Lg onset, and the new Pg onset. Total length of the AR-window: the time difference between the initial Lg onset, and the new Pg onset, plus 5.0 seconds
- FK time window: 0.5 seconds before, and 3.0 seconds after the new Lg onset. Maximum slowness: 0.2, and alpha was set to 6.0, beta was set to 3.46.

Processing details for the ARCES array, Pn phase

- SNR time window: +/- 3.0 seconds from the initial onset.
- Bandpass filter: 4 - 8 Hz.
- AR-coefficients' time window: 4.0 seconds. The time length to look back: 7.0 seconds. Total length of the AR-window: 10.0 seconds.
- FK time window: 0.3 seconds before, and 2.0 seconds after the new Pn onset. Maximum slowness: 0.4.

Processing details for the ARCES array, Sn phase

- SNR time window: + 2.0 seconds after the new Pn onset, to + 5.0 seconds from the initial Sn onset time.
- Bandpass filter: 3 - 5 Hz.
- AR-coefficients' time window: 4.0 seconds. The time length to look back: 6.0 seconds. Total length of the AR-window: 12.0 seconds.
- FK time window: 0.4 seconds before, and 3.0 seconds after the new Sn onset. Maximum slowness: 0.4.

Processing details for the ARCES array, Lg phase

- SNR time window: + 2.0 seconds after the new Sn onset, to + 5.0 seconds from the initial Lg onset time.
- Bandpass filter: 2 - 4 Hz.
- AR-coefficients' time window: 5.0 seconds. The time length to look back: the time difference between the initial Lg onset, and the new Sn onset, minus 3.0 seconds. Total length of the AR-window: 20.0 seconds.
- FK time window: 0.4 seconds before, and 3.0 seconds after the new Lg onset. Maximum slowness: 0.4.

6.4.6 Processing results

Corrections for azimuth and traveltimes

Since we know the locations of the mining events, we could calculate the correct azimuth from the events to the different stations. The mean value and standard deviation of the azimuth residuals were found from taking the mean residual for each mine, and then taking the mean value of all the mines. The mean value and standard deviation of the slowness/velocity were found in a similar way. As the "correct" slowness, we used the value from a local slowness model for the different phases.

The exact origin time for each event was unknown, thus we had to find a way to estimate the origin time. We used the new Pg onset from the Apatity three-component station, APZ9, as an initial value. Then the origin time was derived from a local traveltime model for Pg phases. Since APZ9 is the closest station to the mining events from the Khibiny Massif, we would expect least deviations from the correct Pg onset time for this station. This origin time was then used to derive the mean value and standard deviation of the traveltimes for the phases at the different stations. The mean value and standard deviation for Pg traveltimes for APZ9, were set to the values for the Apatity array, APA0.

The derived corrections for azimuth, slowness and traveltime are given in Tables 6.4.3 to 6.4.5..

Table 6.4.3. Mean value and standard deviation of azimuth residuals.

	Mean (^{0})	std (^{0})
Pg - Apatity array	10.16	3.35
Lg - Apatity array	7.38	4.09
Rg - Apatity array	-1.55	2.34
Pn - ARCES array	4.89	0.52
Sn - ARCES array	3.20	4.43
Lg - ARCES array	-2.9	5.67
Pg - APZ9	6.91	15.09

Table 6.4.4. Mean value and standard deviation of velocity residuals.

	mean (km/s)	std (km/s)
Pg - Apatity array	1.02	0.12
Lg - Apatity array	0.36	0.43
Pn - ARCES array	-0.61	0.06
Sn - ARCES array	-0.47	0.33
Lg - ARCES array	-0.06	0.16
Pg - APZ9	3.75	2.86

Table 6.4.5. Traveltime corrections, mean value and standard deviation.

	mean (s)	std (s)
Pg - Apatity array	-0.13	0.15 (fixed)
Lg - Apatity array	-0.18	1.0 (fixed)
Pn - ARCES array	0.14	0.1 (fixed)
Sn - ARCES array	0.83	0.5 (fixed)
Lg - ARCES array	-2.11	1.0 (fixed)
Pg - APZ9	0.0 (fixed)	0.15 (fixed)
Lg - APZ9	0.22	0.4 (fixed)

Onset time results

From Figs. 6.4.6 to 6.4.8 we can see the results of the automatic processing for the Apatity array, the Apatity three-component station and the ARCES array. In all figures (except Fig. 6.4.6, the line from trace 8: which is the maximum of the STA-envelope) the vertical lines give the minimum of the AR-AIC curve, and thus the new onset time.

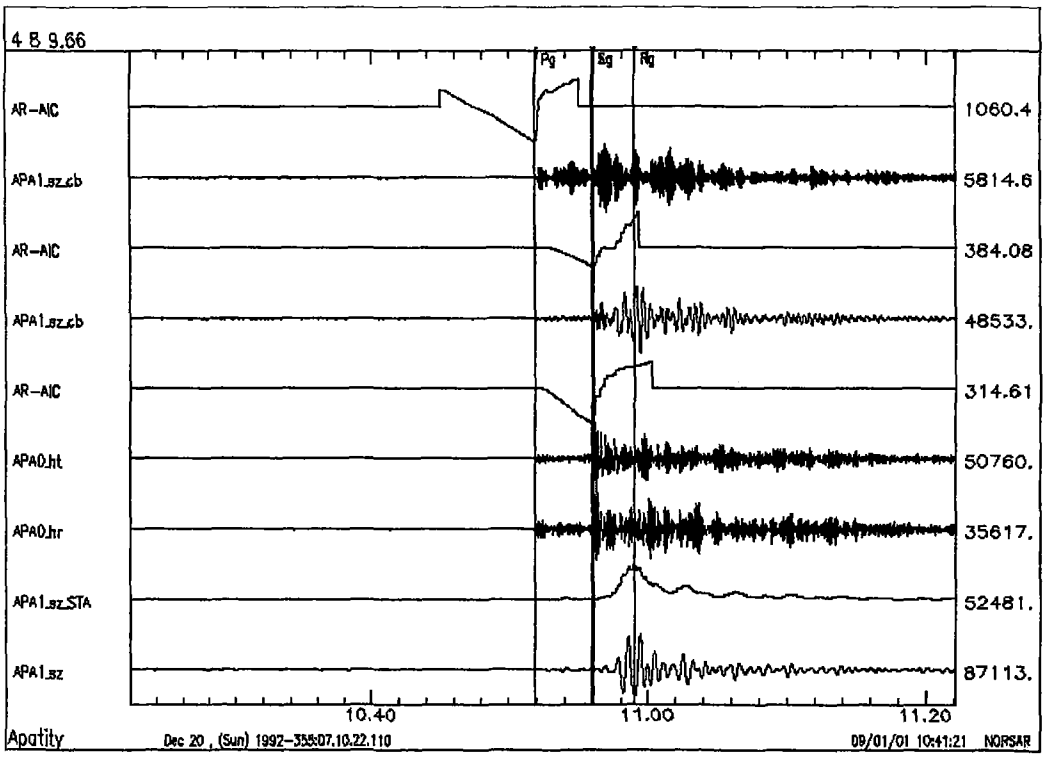

Fig. 6.4.6: Signals from APA0. The 2nd trace from the top is the P-beam filtered in the 4-8 Hz band, with the AR-AIC curve above. The 4th trace is the S-beam filtered in the band 2-8 Hz. The 6th and 7th traces are the rotated, transverse and radial traces from the APA0 three-component seismometer. The 9th trace is the Rg-beam filtered in the band 0.8-2 Hz, with the STA-envelope above it.

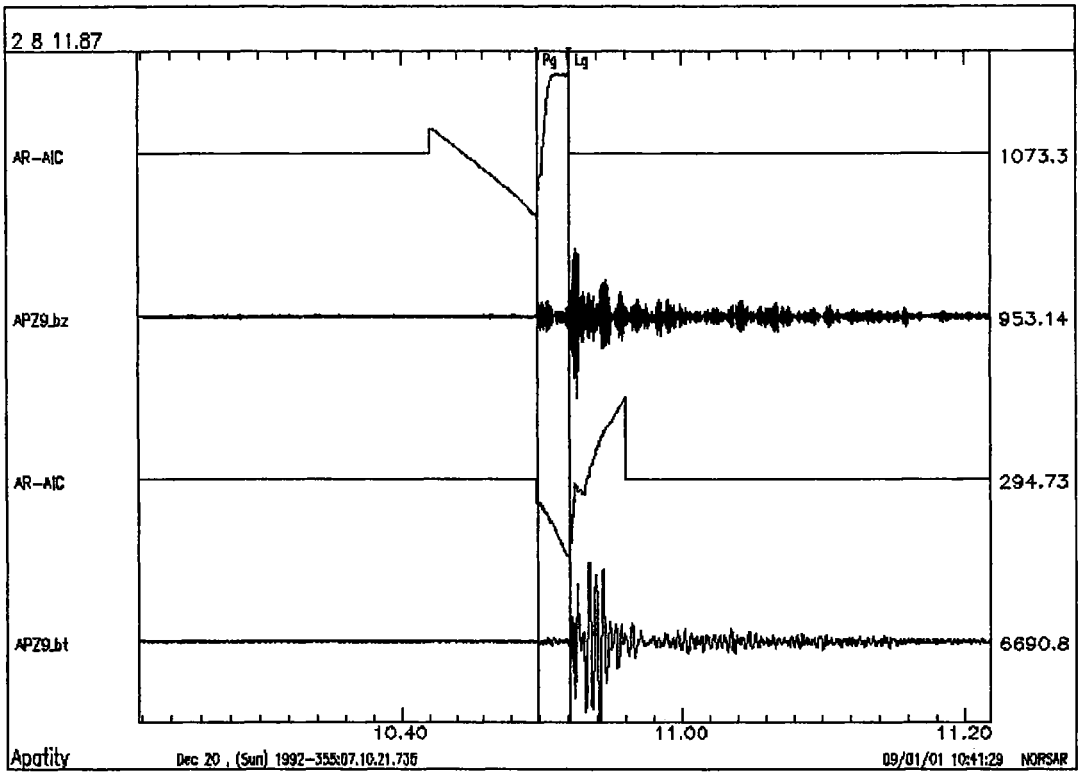

Fig. 6.4.7: Signals from APZ9. The 2nd trace from the top is the vertical trace filtered in the band 4 -8 Hz, with the AR-AIC curve above it. The 4th trace is the rotated, transverse trace filtered in the band 2-8 Hz, with the AR-AIC curve above.

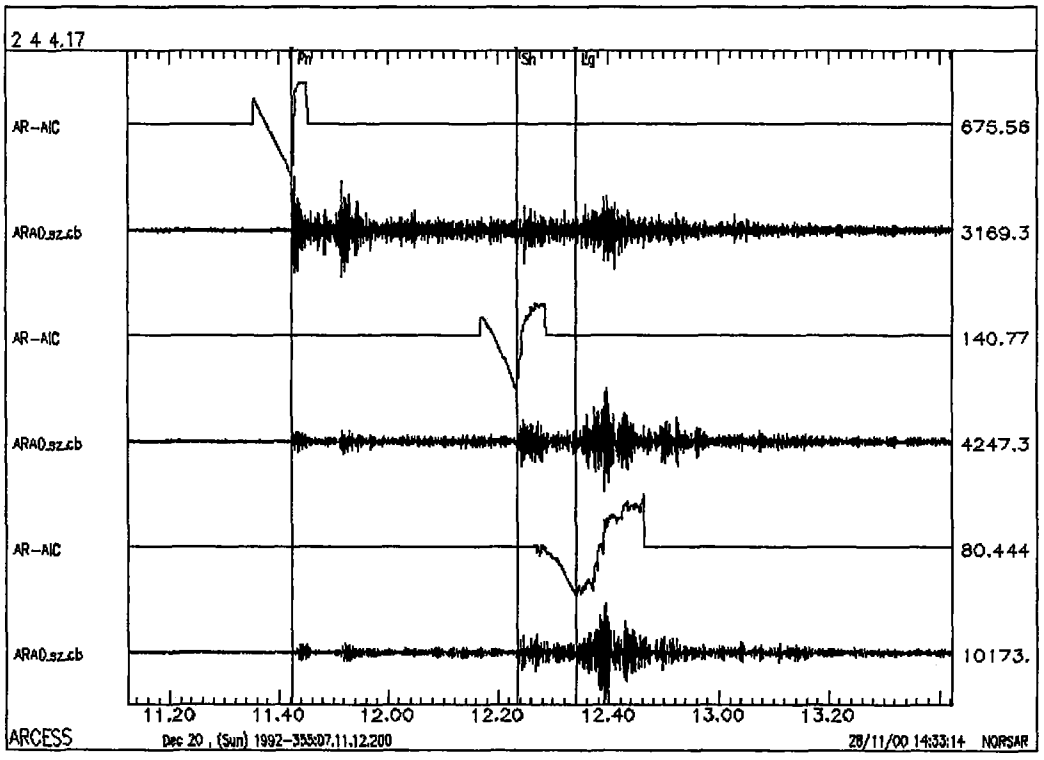

Fig. 6.4.8: Signals from ARCES. The 2nd trace from the top is the P-beam filtered in the band 4-8 Hz, with the AR-AIC curve above it . The 4th trace is the S-beam filtered in the band 3-5 Hz, with the AR-AIC curve above. The 6th trace is S(Lg)-beam filtered in the band 2-4 Hz, with the AR-AIC curve above.

Relocation results of mining events in the Khibiny Massif

After processing of the 36 events from the Khibiny Massif mining area, we have new and improved locations. The new locations are given in Table 6.4.6, and are also seen in Fig. 6.4.9. Compared to Fig. 6.4.5 and Table 6.4.2, the improvement is obvious.

6.4.7 Conclusions

The work so far has been focused on recreating the processing environment used for the original post-processing studies, and adapting this environment to a semi-automatic processing scheme to be applied on a routine basis. As shown in this paper, this has been successfully achieved.

The next step will be to apply the method to other nearby mines, e.g. Kovdor, Zapolyarnyi and Olenegorsk, which are also on the Kola Peninsula, and where our contacts at the Kola Regional Seismological Centre will be in a position to provide us with appropriate ground truth data.

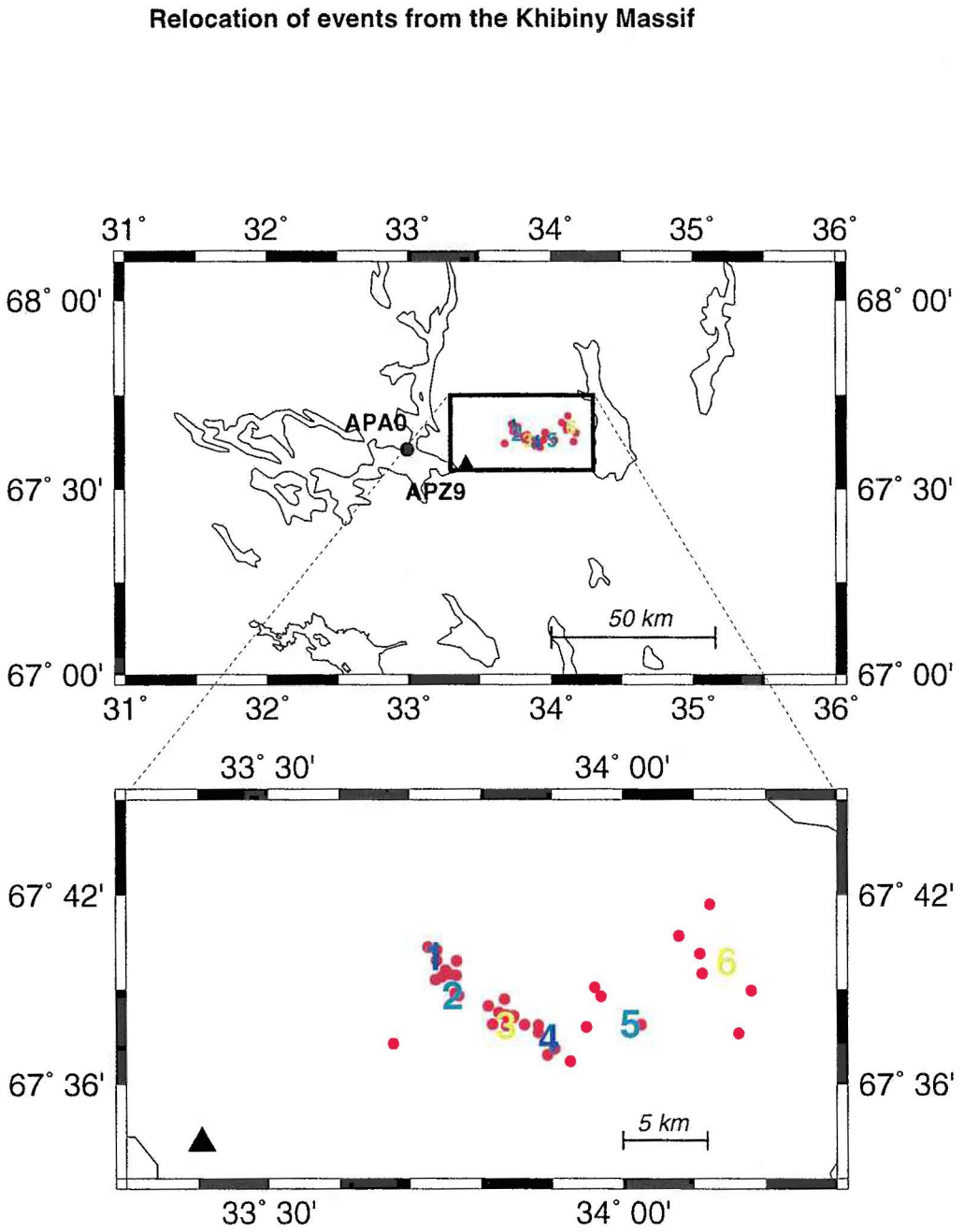

Fig. 6.4.9. The map shows the location of the 36 events after reprocessing the observations as described in the text. The bottom part is an expanded view showing the locations relative to the 6 mines (numbered 1 to 6).

Table 6.4.6. Relocation of the 36 mining events from the Khibiny Massif, with location errors in kilometers (red).

Mine 1	Mine 2	Mine 3	Mine 4	Mine 5	Mine 6
Lat Lon Err (km)	Lat Lon Err (km)	Lat Lon Err (km)	Lat Lon Err (km)	Lat Lon Err (km)	Lat Lon Err (km)
67.6652,33.7387,0.7	67.6445,33.8334,3.1	67.6307,33.8359,0.1	67.6306,33.8809,1.0	67.6510,33.9608,3.0	67.6688,34.1085,1.6
67.6722,33.7264,0.2	67.6551,33.7370,1.4	67.6311,33.8616,1.1	67.6152,33.8941,1.0	67.6462,33.9692,2.4	67.6267,34.1633,4.3
67.6708,33.7386,0.4	67.6476,33.7649,0.2	67.6363,33.8350,0.6	67.6184,33.9038,0.7	67.6311,34.0262,0.7	67.6582,34.1118,1.6
67.6581,33.7560,0.9	67.6313,33.8167,2.9	67.6558,33.8463,2.8	67.6410,33.8109,4.1	67.6300,33.9485,2.7	67.6780,34.0792,3.2
67.6648,33.7668,1.7		67.6374,33.8253,0.8	67.6350,33.8449,2.5		67.6493,34.1804,2.3
67.6600,33.7512,0.6			67.6272,33.8809,0.7		67.6948,34.1225,3.5
67.6466,33.7692,2.3			67.6213,33.6774,9.3		
67.6566,33.7457,0.9			67.6118,33.9258,1.9		
67.6573,33.7658,1.3					

Later, we will expand the processing to other mining areas in Fennoscandia and NW Russia. Eventually, such a two-step reprocessing should be available for the entire European Arctic region covered by the Fennoscandian array network. To apply a similar algorithm on an even broader basis is a natural goal in the long term, but there are many aspects that must be investigated and evaluated before this can be achieved.

We should note that one important reason for the very high location precision obtained for the Khibiny Massif, and documented in this paper, is the geometry of the surrounding array network, in particular the availability of local stations (in Apatity). This situation will of course not be the same for other regions to be processed, and therefore one cannot expect location accuracies as high as 1-2 km on a general basis. Nevertheless, it ought to be possible to improve significantly on the current GBF location precision, which is typically about 20-30 km for "good" solutions and significantly worse in some other cases.

Finally, an interesting project is to evaluate the effect of using "subnetworks" of the available Fennoscandian station network. As is well known, the combination of close-in stations with more remote stations could in some cases make the location less accurate rather than more accurate. We will also study the performance of single-array location relative to network location. This could be useful to develop optimized processing methods for small events, which might be expected to be seen at only one IMS station.

F. Ringdal
T. Kværna
J. Schweitzer
A. Hafslund

References

Fyen, J. (1989): Event Processor program package. *Semiannual Technical Summary, 1989, NORSAR Scientific Report No. 2-88/89.*

GSE/JAPAN/40 (1992): A Fully Automated Method for Determining the Arrival Times of Seismic Waves and its Application to an on-line Processing System.

Kremenetskaya E.O. and V.M.Trjapitsin (1995): Induced seismicity in the Khibiny Massif (Kola Peninsula), *Pure and Applied Geophysics*, **145** No 1, 29-37

Kremenetskaya, E.O.(1991): Contemporary seismicity of the NW part of the USSR, Semian. Tech. Summ., 1 April -30 September 1991, NORSAR Sci.Rep. No 1 -91/92, Kjeller, Norway

Kværna, T. (1990): Generalized Beamforming using a network of four regional arrays. *Semiannual Technical Summary,1990, NORSAR Scientific Report No. 1-90/91.*

Kværna, T. (1993): Intelligent post-processing of seismic events - part 2: Accurate determination of phase arrival times using autoregressive likelihood estimation. *Semiannual Technical Summary,1993, NORSAR Scientific Report No. 2-92/93.*

Kværna, T. (1994): Accurate determination of phase arrival times using autoregressive likelihood estimation. *Annali di Geofisica,* **37**, *287-300*

Kværna, T. and F. Ringdal (1994): Intelligent post-processing of seismic events. *Annali di Geofisica,* **37**, *309-322*

Kværna, T. and F. Ringdal (1996): Generalized beamforming, phase association and threshold monitoring using a global seismic network, in Husebye, E.S. and A.M. Dainty (eds.), Monitoring a Comprehensive Test Ban Treaty, Kluwer Academic Publ., Netherlands, 447-466.

Kværna, T. and D.J. Doornbos (1986): An integrated approach to slowness analysis with arrays and three-component stations. *NORSAR Semiannual Tech. Summ., 1-86/87, NORSAR, Kjeller, 41-50.*

Mykkeltveit, S. (1992): Mining explosions in the Khibiny Massif (Kola Peninsula of Russia) recorded at the Apatity three-component station, Report PL-TR-92-2253, Phillips Laboratory, Hanscom Air Force Base, MA, USA.

Mykkeltveit, S. and F. Ringdal (1981): Phase identification and event location at regional distances using small-aperture array data, in *Identification of Seismic Sources -- Earthquake or underground Explosions,* E.S. Husebye and S. Mykkeltveit, eds. Dordrecht, Holland, 467-481.

Mykkeltveit, S. and H. Bungum (1984): Processing of seismic events using data from small-aperture arrays. *Bull. Seism. Soc. Am.* **74**, *2313-2333.*

Ringdal, F. and T. Kværna, (1989): A multichannel processing approach to real time network detection, phase association and threshold monitoring. *Bull. Seism. Soc. Am.* **79**, *1927-1940.*

Schweitzer, J., (2001): HYPOSAT - An Enhanced Routine to Locate Seismic Events. *Pure and Applied Geophysics,* **158**, 277-289.

Yokota, T., S. Zhou, M.Mizoue and I. Nakamura (1981): An automatic measurement of arrival time of seismic waves and its application to an on-line processing system (in Japanese with English abstract), *Bull. earthquake Res. Inst. Univ. Tokyo,* **55**, *449-484.*